

Coherent Excitation with Phase-Incremented Pulses

Shanmin Zhang and David G. Gorenstein

Sealy Center for Structural Biology and the Department of Human Biological Chemistry and Genetics, University of Texas Medical Branch, Galveston, Texas 77555-1157

E-mail: shanmin@tesla.utmb.edu

Received June 28, 2001; revised September 21, 2001; published online November 29, 2001

An outline is given for calculating the evolution of a spin system by a pulse sequence with phase-incremented pulses (PIPs). It is done in a frame with a speed of $2\pi\Delta f = \Delta\varphi/\Delta\tau$ relative to the rotating frame, where $\Delta\varphi$ and $\Delta\tau$ are the phase- and time-increment of the PIP. This particular frame is defined as the eigenframe, in which the phase of the PIP for the center band is stationary and is subjected to a universal phase shift ($\text{UPS} = -\Delta\varphi/2$), and the strength of the PIP is scaled by a factor of $\lambda = \sqrt{2[1 - \cos(\Delta\varphi)]}/|\Delta\varphi|$. The phase differences between different eigenframes can be attributed to the initial phases of the PIPs, making it possible to use the Bloch vector model even in different eigenframes. A new way is provided to construct composite pulses with not only amplitude and phase modulations but also offset modulation. Several examples, including a broadband inversion pulse, a Hahn spin echo, and a selective inversion and null pulse, all composed of PIPs, are discussed in detail. © 2002 Elsevier Science

Key Words: coherent excitation; phase-incremented pulse; universal phase shift; scaling factor of pulse strength; phase inheritance.

INTRODUCTION

Phase-incremented pulse (I - δ) (PIP) is used commonly in multidimensional NMR experiments (7 - 10) to achieve frequency-shifted (or jumped) excitation usually in the ^{13}C channel at high field. Unlike a real jump of the carrier frequency in some of the NMR experiments, PIPs will not distort the phase coherence between the RF pulses applied before and after PIPs. The PIPs require almost no delay and have no noticeable phase glitches for modern NMR instruments. Also, the amount of frequency shift Δf can be made sufficiently large to cover the entire range of the ^{13}C chemical shift even at the highest magnetic field available now.

Often PIP is adapted in a noncoherent way; i.e., the phase of the pulse plays no role in the experiments. For example, a frequency-shifted selective inversion of $^{13}\text{C}_\alpha$ spins in the middle of the ^{13}CO evolution for homonuclear decoupling has no restriction on the phase of the pulse. Things become quite different when coherent excitation, with a number of PIPs, is required. One faces a special case where a spin experiences an on-resonance excitation but off-resonance evolution in the (con-

ventional) rotating frame (II). It is more intriguing if different PIPs have different frequency shifts. Under such a circumstance, the evolution of a spin system has to be calculated in different rotating frames, in which the phase relationship and the offsets must be taken into account cautiously.

The phase coherence between pulses and scans is critical in NMR experiments. It is maintained through a reference signal (Fig. 1) that provides a phase reference for all the pulses applied at any time. For example, if the first pulse, described by $A_{\max} \sin(\omega_{\text{rf}}t)$, is applied at a time $t = 0$, the second pulse, applied at a time t_s from the beginning of the pulse sequence, must have the form of

$$A_{\max} \sin[\omega_{\text{rf}}(t - t_s) + \varphi_s], \quad t_s \leq t, \quad [1]$$

in order to keep the same phase as the first one. In Eq. [1], $\varphi_s = \omega_{\text{rf}}t_s$ is inherited from the reference signal as shown in Fig. 1. It can be considered that the first pulse is extended continuously to the second one with zero amplitude in the pulse interval. Little attention has been paid to the phase inheritance in NMR experiments since the NMR instrument takes care of it automatically for users.

For a frequency-shifted excitation by a PIP (Fig. 2), the effective carrier frequency $\omega_{\text{rf}}/2\pi$ (or the on-resonance) is shifted to $\Delta f + \omega_{\text{rf}}/2\pi$. Therefore, the phase of the PIP should be defined in a rotating frame with a speed of $2\pi\Delta f$ relative to the rotating frame since only in this frame is the phase of the PIP for the center band stationary (Fig. 2). This particular rotating frame is defined as the eigenframe of the PIP, where the evolution of the density operator can be calculated as if in the rotating frame. For more than one PIP, the phase inheritance must also be satisfied as in the case of the RF pulses (Fig. 3) to maintain phase coherence. For the most simplified phase inheritance with two consecutive PIPs, the phase of the first increment of the PIP₂ must have a value that is one increment $\Delta\varphi$ greater than the phase of the last step of the PIP₁ in order to keep the same phase of the two PIPs, where phase increment $\Delta\varphi$ is the same for both PIPs. The phase inheritance for PIPs will be defined in a broader way in the following.

In this contribution, an outline for calculating the evolution of a spin system by phase-incremented pulses (PIPs) will be

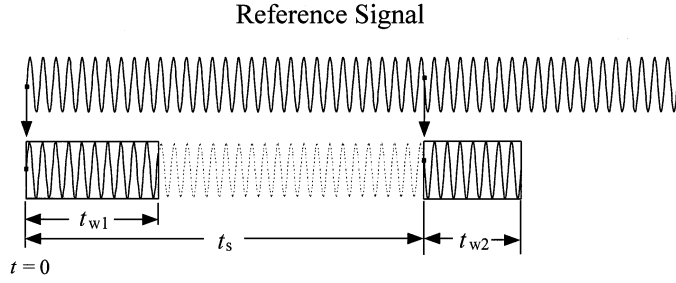


FIG. 1. A reference signal (top) used as a phase reference for RF pulses applied at any time. The initial phases of the first and second pulses are inherited from the reference signal at time $t = 0$ and $t = t_s$, respectively. Consequently, both pulses have the same phase.

presented first, and it is then applied to calculate a number of sequences composed of PIPs.

OUTLINE OF CALCULATION

A spin system initially in thermal equilibrium is usually described by a density operator $\sigma(0)$, which is proportional to I_z under the high temperature approximation (12). After a 90° pulse, the system will evolve under the Hamiltonian, and the density operator $\sigma(t)$ in the rotating frame with a speed of the carrier frequency ($\omega_{rf}/2\pi$) can be written as (12, 13)

$$\sigma(t) = L(t)\sigma(0)L^{-1}(t), \quad [2]$$

where the unitary propagator is defined as

$$L(t) = Te^{-i \int_0^t \mathcal{H}(t') dt'}, \quad [3]$$

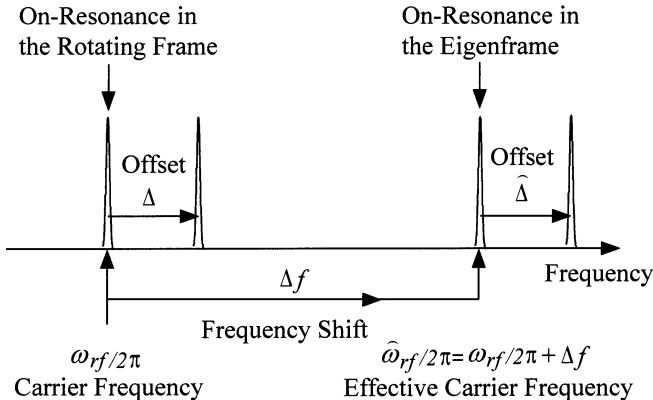


FIG. 2. The relationship between the excitations in the rotating frame by a RF pulse and in the eigenframe by a PIP. The offset in the eigenframe $\hat{\Delta}$ is measured from the effective carrier $\hat{\omega}_{rf}/2\pi = \Delta f + \omega_{rf}/2\pi$, where the frequency shift $\Delta f = \Delta\varphi/2\pi \Delta\tau$.

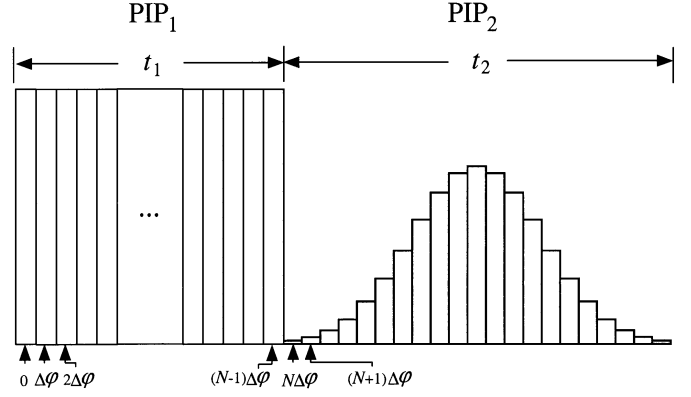


FIG. 3. Schematic representation of the phase inheritance for two PIPs applied consecutively with the same phase increment $\Delta\varphi$ and time increment $\Delta\tau$.

and T is the Dyson time ordering operator. The Hamiltonian of the system in the rotating frame can be expressed as

$$\mathcal{H}(t) = (\omega_0 - \omega_{rf})I_z + \mathcal{H}_{in} + \omega_1(t) \cdot I, \quad [4]$$

where the chemical-shift term for a particular resonance frequency $\omega_0/2\pi$ is shown explicitly for simplicity and the truncated time-independent internal Hamiltonian \mathcal{H}_{in} includes all the other spin interactions, J coupling for instance. $\omega_1(t)$ in Eq. [4] represents the strength and phase of the RF field.

For a phase-incremented pulse, the last term in Eq. [4] can be expressed as

$$\omega_1(t) \cdot I = \omega_1(t)e^{-i[\varphi_0 + \varphi(t)]I_z} I_x e^{i[\varphi_0 + \varphi(t)]I_z}, \quad [5]$$

where φ_0 is the initial phase, and $\varphi(t)$ is the phase that increments, i.e.,

$$\varphi(t) = \begin{cases} 0, & 0 \leq t < \Delta\tau \\ \Delta\varphi, & \Delta\tau \leq t < 2\Delta\tau \\ 2\Delta\varphi, & 2\Delta\tau \leq t < 3\Delta\tau \\ \dots & \dots \\ (N-2)\Delta\varphi, & (N-2)\Delta\tau \leq t < (N-1)\Delta\tau \\ (N-1)\Delta\varphi, & (N-1)\Delta\tau \leq t \leq N\Delta\tau, \end{cases} \quad [6]$$

where N is the number of steps of the PIP and $-\pi < \Delta\varphi \leq \pi$. In general, any PIP (Fig. 3) can be represented by the notation of $\text{PIP}\Delta f(\varphi_0, \Delta\varphi, \Delta\tau, \omega_1(t), \text{steps})$, where Δf , φ_0 , $\Delta\varphi$, $\Delta\tau$, and $\omega_1(t)$ are the frequency shift (in kHz), initial phase, phase increment, time increment, and pulse strength, respectively. The frequency shift of the center band is well known (1, 3–6),

$$\Delta f = \frac{\Delta\varphi}{2\pi \Delta\tau}, \quad [7]$$

as shown in Fig. 2.

PIP also excites multiple unsymmetrical sidebands (6) located at $j/\Delta\tau$ ($j = \pm 1, \pm 2, \dots$) from the center band. For a sufficiently small $\Delta\tau$, the sidebands are far outside of the spectral width where there are usually no NMR peaks at all. Consequently, the sideband excitations have little effect on the center band and therefore will be neglected in the following.

Due to the complication of the PIPs, any attempt trying to solve Eq. [2] in the rotating frame is rather discouraging. It is, however, quite intuitive to introduce a new rotating frame with a speed of

$$\widehat{\omega} = 2\pi\Delta f = \frac{\Delta\varphi}{\Delta\tau}, \quad [8]$$

relative to the rotating frame. Only in this eigenframe (denoted by the symbol \sim) is the phase of the PIP a constant.

The Hamiltonian in Eq. [4] can be transferred into the eigenframe with a unitary operator $U = e^{-i\widehat{\omega}tI_z}$ (6, 11)

$$\begin{aligned} \widehat{\mathcal{H}}(t) &= U^{-1}\mathcal{H}U - iU^{-1}\dot{U} \\ &= (\Delta\omega - \widehat{\omega})I_z + \widehat{\mathcal{H}}_{in} + \omega_1(t)e^{i\widehat{\omega}tI_z} \\ &\quad \times [e^{-i[\varphi_0+\varphi(t)]I_z}I_x e^{i[\varphi_0+\varphi(t)]I_z}]e^{-i\widehat{\omega}tI_z} \\ &\approx \Delta\widehat{\omega}I_z + \mathcal{H}_{in} + \lambda\omega_1(t)e^{-i(\varphi_0-\frac{\Delta\varphi}{2})I_z}I_x e^{i(\varphi_0-\frac{\Delta\varphi}{2})I_z}, \quad [9] \end{aligned}$$

where $\Delta\omega/2\pi = (\omega_0 - \omega_{rf})/2\pi$ is the offset in the rotating frame, $\Delta\widehat{\omega}/2\pi = (\omega_0 - \omega_{rf} - \widehat{\omega})/2\pi$ is the offset in the eigenframe (Fig. 2), λ is a scaling factor of the RF field strength (defined in Eq. [11]), and $-\Delta\varphi/2$ is a phase shift (defined in Eq. [12]). In Eq. [9], $\widehat{\mathcal{H}}_{in} = \mathcal{H}_{in}$ since the truncated internal interaction commutes with I_z , i.e., $[\mathcal{H}_{in}, I_z] = 0$.

As shown in Fig. 4, the phase of the RF field in the eigenframe, $\widehat{\varphi}(t) = (\Delta\varphi/2)[1 - (2t/\Delta\tau)]$ for $0 \leq t \leq \Delta\tau$, is periodic and the effective field for the center band excitation can be expressed as (6)

$$\begin{aligned} \frac{\omega_1 \cdot \mathbf{I}}{2\pi} &= \frac{f_1}{\Delta\tau} \int_0^{\Delta\tau} \{I_x \cos[\widehat{\varphi}(t)] + I_y \sin[\widehat{\varphi}(t)]\} dt \\ &= \frac{\sqrt{2[1 - \cos(\Delta\varphi)]}}{|\Delta\varphi|} f_1 I_x, \quad [10] \end{aligned}$$

which implies that the RF field strength is scaled by a factor of

$$\lambda = \frac{\sqrt{2[1 - \cos(\Delta\varphi)]}}{|\Delta\varphi|}. \quad [11]$$

Equation [10] is equivalent to taking a zero-order averaging of the interaction in the eigenframe.

A phase shift is also introduced in the eigenframe (Fig. 4), which is termed the universal phase shift (UPS) and exists in all

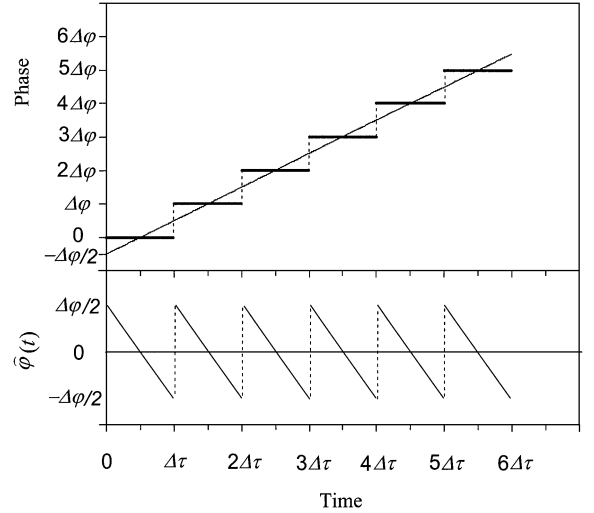


FIG. 4. (Top) The phases of a phase-incremented pulse (step function), with a time increment of $\Delta\tau$ and phase increment of $\Delta\varphi$, and of a phase linearly, continuously increased pulse (straight line) in the rotating frame. The two phases of the pulses cross in the middle of each increment, leading to an initial phase shift of $-\Delta\varphi/2$ for the phase continuous pulse. (Bottom) The phase of the phase-incremented pulse in the eigenframe with a speed of $\widehat{\omega} = \Delta\varphi/\Delta\tau$ relative to the rotating frame. It is the difference between the two phases shown on the top.

sideband excitations (6),

$$\text{UPS} = -\frac{\Delta\varphi}{2}. \quad [12]$$

The definitions of λ and UPS are slightly different from the previous article (6), where, for $\Delta\varphi < 0$, $\lambda (= \sqrt{2[1 - \cos(\Delta\varphi)]}/\Delta\varphi)$ becomes negative and UPS ($= -\pi - \Delta\varphi/2$) includes a $-\pi$. However, the overall effect is the same.

The evolution of the density operator can be calculated in the eigenframe first and it is then transferred into the rotating frame. For a pulse sequence of any number of PIPs, the density operator is described by

$$\begin{aligned} \sigma(t_1 + t_2 + \dots + t_n) &= U_n \dots U_2 U_1 \widehat{\mathbf{L}}_n(t_n) \dots \widehat{\mathbf{L}}_2(t_2) \widehat{\mathbf{L}}_1(t_1) \sigma(0) \\ &\quad \times \widehat{\mathbf{L}}_1^{-1}(t_1) \widehat{\mathbf{L}}_2^{-1}(t_2) \dots \widehat{\mathbf{L}}_n^{-1}(t_n) U_1^{-1} U_2^{-1} \dots U_n^{-1}, \quad [13] \end{aligned}$$

where the shifted-propagator $\widehat{\mathbf{L}}_k(t_k)$ ($k \neq 1$) in the eigenframe is defined as

$$\begin{aligned} \widehat{\mathbf{L}}_k(t_k) &= U_1^{-1} U_2^{-1} \dots U_{k-1}^{-1} \widehat{\mathbf{L}}_k(t_k) U_{k-1} \dots U_2 U_1 \\ &= \mathcal{T} e^{-i \int_0^{t_k} U_1^{-1} U_2^{-1} \dots U_{k-1}^{-1} \widehat{\mathcal{H}}_k(t') U_{k-1} \dots U_2 U_1 dt'} \\ &= \mathcal{T} e^{-i \int_0^{t_k} \widehat{\mathcal{H}}_k(t') dt'}. \quad [14] \end{aligned}$$

In the above equation,

$$\begin{aligned} \widehat{\mathcal{H}}_k(t) = & \Delta \widehat{\omega}_k I_z + \mathcal{H}_{in} \\ & + \lambda_k \omega_{1k}(t) e^{-i(\varphi_{0k} + \text{UPS}_k - \phi_{k-1})I_z} I_x e^{i(\varphi_{0k} + \text{UPS}_k - \phi_{k-1})I_z} \end{aligned} \quad [15]$$

is the shifted-Hamiltonian of the PIP_k in the eigenframe, and

$$\phi_{k-1} = \widehat{\omega}_1 t_1 + \widehat{\omega}_2 t_2 + \cdots + \widehat{\omega}_{k-1} t_{k-1} \quad [16]$$

is the sum of all the phases accumulated through the changes of the eigenframes before the PIP_k.

The phase of the PIP_k (Eq. [15]),

$$\varphi_k = \varphi_{0k} + \text{UPS}_k - \phi_{k-1}, \quad [17]$$

is determined not only by its own initial phase φ_{0k} and UPS_k but also by an inherited phase ϕ_{k-1} from all the previous PIPs. Equation [17] is a more general expression of the phase inheritance for any PIP. Unlike the normal RF pulses, this phase inheritance must be taken care of by the user rather than by the NMR instrument. To have a desired phase φ_k of the PIP_k, the initial phase φ_{0k} can be adjusted.

Equation [13] allows us to calculate the response of a spin system by any number of PIPs. The unitary operators $U_1^{-1} U_2^{-1} \cdots U_{k-1}^{-1}$ act on the propagator \widehat{L}_k (Eq. [14]), causing only a phase shift of the PIP_k (Eq. [15]). The shifted propagators $\widehat{L}_k \cdots \widehat{L}_2 \widehat{L}_1$ act consecutively on the density operator without the frame transfer as if in the rotating frame with a single carrier. The offset, however, must be calculated in the eigenframe of each PIP_k, i.e., $\Delta \widehat{\omega}_k / 2\pi = (\omega_0 - \omega_{rf} - \widehat{\omega}_k) / 2\pi$.

It is worth mentioning that Eq. [13], derived from the PIPs, is actually rather general and can be used for any pulse sequences with or without PIPs. If $\Delta\varphi$ of a PIP equals zero, the PIP $\Delta f(\varphi_0, \Delta\varphi = 0, \Delta\tau, \omega_1(t), \text{steps})$ reduces to a normal pulse. If, on the other hand, $\omega_1 = 0$ (correspondingly, $\varphi_0 = 0$ and $\Delta\varphi = 0$), the PIP reduces to a delay with a delay time equal to the pulse width. Equation [13] can also be applied to pulse sequences with a real jump of a carrier frequency if the phase change resulted from each frequency jump is known.

APPLICATIONS

To show the applications of the above results, three experiments are discussed. Two of them, a broadband inversion and a Hahn spin echo, are well known and described in the rotating frame. They need modifications in order to work in the eigenframe. The third one is a composite pulse with offset modulation.

Assume a broadband inversion pulse (14) ($90_x 180_y 90_x$) is adapted to excite a region 50 kHz away from the carrier frequency. The three RF pulses are replaced by three PIPs. The PIP₁ has 50 steps, a time increment $\Delta\tau = 0.5 \mu\text{s}$, and a phase increment $\Delta\varphi = 9^\circ$ that is determined from Eq. [7]. The pulse can be represented by PIP₁50($4.5^\circ, 9^\circ, 0.5 \mu\text{s}, 10.01 \text{ kHz}, 50$),

where the RF field strength 10.01 kHz is calculated from the 90° pulse width ($25 \mu\text{s}$) and the scaling factor λ ($= 0.99897$). An initial phase $\varphi_0 = 4.5^\circ$ is used in the PIP₁ to compensate the $\text{UPS}_1 = -(1/2)\Delta\varphi = -4.5^\circ$, otherwise the PIP₁ would have a phase of -4.5° rather than 0° (or the x phase).

To achieve the same frequency shift as the PIP₁, the PIP₂ and PIP₃ have the same $\Delta\tau$, $\Delta\varphi$, and the pulse strength as the PIP₁. Since the PIP₂ is a 180° pulse, it has 100 steps. In addition to its own UPS_2 ($= -4.5^\circ$), the PIP₂ is also subjected to an inherited phase ϕ_1 ($= \widehat{\omega}_1 t_1 = 450^\circ$) (Eq. [16]). To construct the PIP₂ with a 90° (or y) phase, the phase inheritance requires (Eq. [17])

$$\varphi_2 = \varphi_{02} + \text{UPS}_2 - \phi_1 = 90^\circ, \quad [18]$$

from which we get $\varphi_{02} = 184.5^\circ$. The PIP₂ can be expressed as PIP₂50($184.5^\circ, 9^\circ, 0.5 \mu\text{s}, 10.01 \text{ kHz}, 100$). Similarly, PIP₃ can be determined as PIP₃50($-85.5^\circ, 9^\circ, 0.5 \mu\text{s}, 10.01 \text{ kHz}, 50$). Here the final frame transfer to the rotating frame λ using $U_3 U_2 U_1$ (Eq. [13]) is not necessary since only the inversion profile (or the z component of the magnetization) is of interest.

The simulated broadband inversion profile by the three PIPs is shown in Fig. 5a, resembling the profile by the composite pulse $90_x 180_y 90_x$ except for different excitation regions. Figure 5b shows the profile by the same composite PIP but different initial phases, $\varphi_{01} = 0^\circ$, $\varphi_{02} = 90^\circ$, and $\varphi_{03} = 0^\circ$, which are used in the original composite pulse. The inversion profile is distorted severely, showing that the right phase relationship in the rotating frame is a wrong one in the eigenframe.

For a Hahn spin-echo sequence (15), $90_y - \tau - 180_x - \tau'$, the magnetization in the rotating frame will be refocused to the x axis at the end of the sequence. To create a spin echo 50 kHz away from the carrier frequency, two PIPs are required. The first 90_y

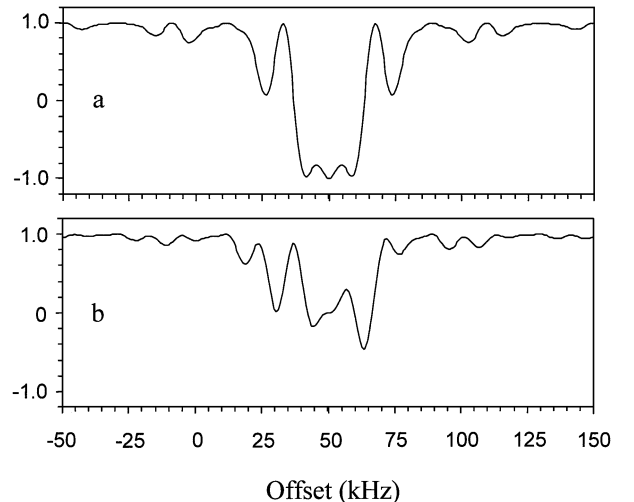


FIG. 5. Simulated broadband inversion profiles by a composite (180°) PIP (a), PIP₁50($4.5^\circ, 9^\circ, 0.5 \mu\text{s}, 10.01 \text{ kHz}, 50$) PIP₂50($184.5^\circ, 9^\circ, 0.5 \mu\text{s}, 10.01 \text{ kHz}, 100$) PIP₃50($-85.5^\circ, 9^\circ, 0.5 \mu\text{s}, 10.01 \text{ kHz}, 50$), and by the same PIPs but different initial phases (b), $\varphi_{01} = 0^\circ$, $\varphi_{02} = 90^\circ$, and $\varphi_{03} = 0^\circ$.

pulse can be replaced by PIP₁50(94.5°, 9°, 0.5 μs, 10.01 kHz, 50), where the same parameters as the previous case are used. A 4.5° phase is included in the initial phase to compensate the UPS (= -(1/2)Δφ = -4.5°). After the PIP₁ there is a delay τ, during which the evolution of the density operator can still be considered in the eigenframe, as if the PIP₁ were extended to the entire τ with zero pulse strength. The initial phase φ₀₂ of the PIP₂ should satisfy the phase inheritance φ₂ = φ₀₂ + UPS₂ - φ₁ = 0° in order to refocus the magnetization to the x axis in the eigenframe. However, to refocus the final magnetization to the x axis in the rotating frame, the density operator in the eigenframe needs to be transferred back to the rotating frame (Eq. [13]), which introduces an additional phase shift of ω̄(3t_w + τ + τ') (t_w represents the pulse width of the PIP₁). To compensate this phase shift, the magnetization should be refocused to an axis with a phase of -ω̄(3t_w + τ + τ') rather than to the x axis in the eigenframe. This can be accomplished by adding a phase of -ω̄(3t_w + τ + τ')/2 to φ₂ of the PIP₂, leading to the phase inheritance of

$$\varphi_2 = \varphi_{02} + \text{UPS}_2 - \phi_1 = -\bar{\omega}(3t_w + \tau + \tau')/2, \quad [19]$$

or

$$\begin{aligned} \varphi_{02} &= \bar{\omega}(t_w + \tau) + \frac{\Delta\varphi}{2} - \frac{\bar{\omega}}{2}(3t_w + \tau + \tau') \\ &= \frac{\Delta\varphi}{2} - \frac{\bar{\omega}}{2}(\tau' - \tau + t_w). \end{aligned} \quad [20]$$

For τ' = τ,

$$\varphi_{20} = \frac{\Delta\varphi}{2} - \frac{\bar{\omega}}{2}t_w, \quad [21]$$

where the delay and the pulse width of the PIP₂ disappear due the refocusing nature of the 180° pulse. Only the UPS (= -Δφ/2) and the phase -ω̄t_w/2 (partially refocused) need to be taken into account. From Eq. [21], the initial phase of the PIP₂ can be determined, φ₂₀ = -220.5° or 139.5°. The PIP₂ is then PIP₂50(139.5°, 9°, 0.5 μs, 10.01 kHz, 50).

For τ' = τ - t_w, however,

$$\varphi_{02} = \frac{\Delta\varphi}{2}, \quad [22]$$

which is now independent of the pulse width t_w and delay τ. For sufficiently small phase increment Δφ, the phase relationships of the two pulses, in the rotating frame and in the eigenframe, become the same.

In many triple-resonance experiments, HNC0 for example, coherence needs to be transferred from the amide ¹⁵N to the adjacent ¹³CO but not to the ¹³C_α. For this purpose, a ¹³CO 180° pulse is used in the INEPT segment, which inverts the ¹³CO region centered at 174 ppm but nulls the ¹³C_α region centered at

56 ppm. To achieve this, the RF field strength must satisfy the relationships of (7)

$$2\pi f_1 t_w = \pi, \quad \text{for inversion of } ^{13}\text{CO} \quad [23]$$

and

$$2\pi\sqrt{f_1^2 + \Delta^2}t_w = 2m\pi, \quad \text{for null of } ^{13}\text{C}_\alpha, \quad [24]$$

which leads to

$$f_1 = \frac{\Delta}{\sqrt{4m^2 - 1}}, \quad [25]$$

where Δ(≈118 ppm) is the difference of chemical shifts between the centers of ¹³CO and ¹³C_α. For m = 1, corresponding to a 2π rotation of ¹³C_α, Eq. [25] reduces to

$$f_1 = \frac{\Delta}{\sqrt{3}}. \quad [26]$$

The inversion and null profiles of this scheme are shown in Fig. 6a. It has a narrow inversion and null bandwidths and the null point moves when f₁ varies.

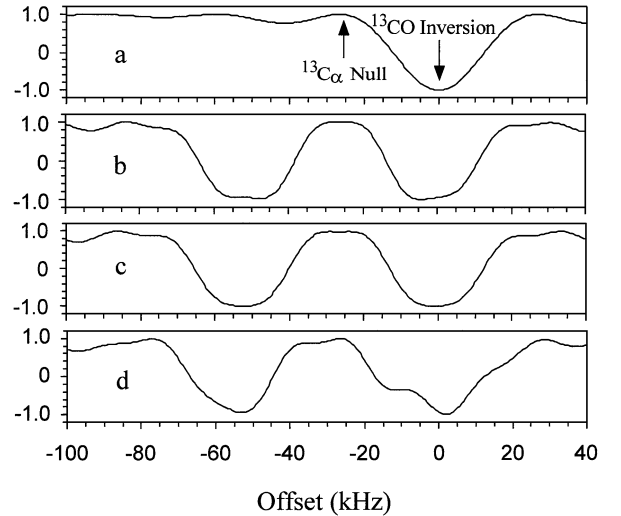


FIG. 6. Simulated excitation profiles of selective inversion and null by a single RF pulse (a) and by two PIPs (b, c, and d). The single pulse is applied on-resonance to the center of the ¹³CO region (174 ppm, assigned to 0 kHz) with a pulse strength f₁ = 15.42 kHz and pulse width t_w = 32.4 μs. Under this condition, the center of the ¹³C_α region (56 ppm, corresponding to -26.7 kHz at the 900-MHz field) is subjected to a 2π rotation, resulting in a null excitation as shown in (a). For (b), two consecutive PIPs, PIP₁0(0°, 0°, 0.6 μs, 15.42 kHz, 54) and PIP₂-53.4(5.77°, -11.54°, 0.6 μs, 15.42 kHz, 54), are used with the PIP₁0 being the same as the RF pulse used in (a) and the PIP₂53.4 being a compensating pulse. Profile (c) is obtained by adjusting slightly the center of inversion and the overall rotation angle. The two PIPs used are PIP₁1.57(0.17°, 0.34°, 0.6 μs, 18.34 kHz, 51) and PIP₂-54.95(11.36°, -11.87°, 0.6 μs, 18.34 kHz, 51). The compensation becomes rather poor (d) by exchanging the order of the two PIPs used in (b) due to the failure of the phase-inheritance.

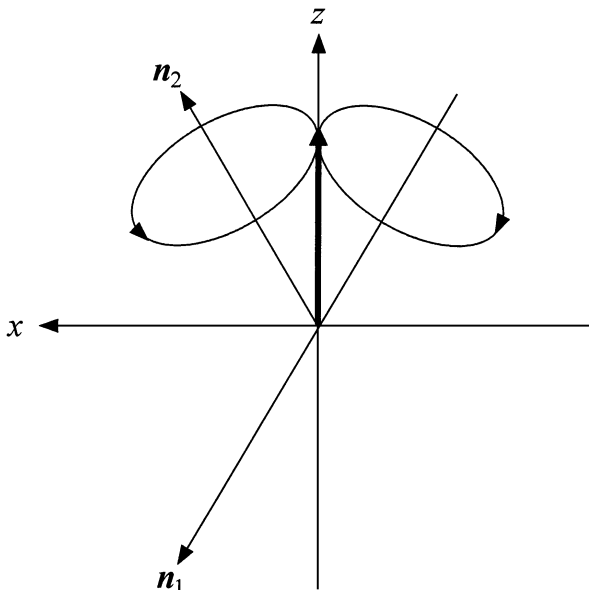


FIG. 7. Offset compensated two consecutive 2π rotations by two PIPs around n_1 in the eigenframe of the PIP₁ with a negative offset $-\bar{\Delta}$ and around n_2 in the eigenframe of the PIP₂ with a positive offset $\bar{\Delta}$. Both pulses have an x phase but in different eigenframes.

To overcome these problems, a compensating pulse can be applied on the other side of the $^{13}\text{C}_\alpha$ region with a PIP. Since the effective carrier frequency shifts from one side of the $^{13}\text{C}_\alpha$ region to the other, the effective offset $\bar{\Delta}$ in the eigenframe changes sign. With the compensating pulse, the center of $^{13}\text{C}_\alpha$ is subjected to two consecutive 2π rotations of opposite offsets, one positive and the other negative, but of the same (x) phases in the two different eigenframes, as shown in Fig. 7. In the vicinity of the center of $^{13}\text{C}_\alpha$, the sum of the two rotation angles can be expressed as

$$\varphi = 2\pi\sqrt{f_1^2 + (\bar{\Delta} - \delta)^2}t_w + 2\pi\sqrt{f_1^2 + (\bar{\Delta} + \delta)^2}t_w, \quad [27]$$

where δ is an offset measured from the center of $^{13}\text{C}_\alpha$. For small δ (compared with $\bar{\Delta}$), Eq. [27] can be expanded in a series of δ ,

$$\begin{aligned} \varphi &= 2\pi\sqrt{f_1^2 + \bar{\Delta}^2}t_w - 2\pi\frac{\bar{\Delta}t_w}{\sqrt{f_1^2 + \bar{\Delta}^2}}\delta + \dots \\ &\quad + 2\pi\sqrt{f_1^2 + \bar{\Delta}^2}t_w + 2\pi\frac{\bar{\Delta}t_w}{\sqrt{f_1^2 + \bar{\Delta}^2}}\delta + \dots \\ &= 4\pi\sqrt{f_1^2 + \bar{\Delta}^2}t_w + \dots \approx 4\pi. \end{aligned} \quad [28]$$

In the above equation, the first-order terms in δ cancel, which implies that the deviation from a 360° rotation of the PIP₁ due to a small δ is compensated by the deviation of the PIP₂. To the first order of δ , the rotation angle $\varphi \approx 4\pi$, leading to a re-

markable compensation. As a consequence, the null point at the $^{13}\text{C}_\alpha$ region is broadened significantly (Fig. 6b). It is important to note that the inversion region of ^{13}CO is broadened as well by the compensating PIP₂ (Fig. 6b) since the overall rotation angle and axis by the two PIPs become quite insensitive to the offsets. It is calculated that the overall rotation angle at the center of ^{13}CO is about 161.46° rather than 180° but the rotation axis is approximately in the $x - y$ plane, causing an incomplete inversion. Also the center of inversion is slightly shifted to the upfield region. These effects are caused by the interference between the two bands and will disappear if the separation between the two bands is much greater than the RF field strength. It can be shown that the overall rotation becomes 179.97° when the RF field strength is increased to $2\pi f_1 t_w = 202^\circ$. The small shift of the inversion center can be corrected by adding a small phase increment to the PIP₁. The final result is shown in Fig. 6c.

As shown in Fig. 6d, the compensating effect becomes quite poor when the order of the two PIPs is changed due to the failure of the phase-inheritance mentioned above.

The excitation in the middle can also be compensated by applying two identical pulses simultaneously, one at the offset Δ and the other at $-\Delta$, as used in homonuclear decoupling to compensate the Bloch–Siegert shift (16, 17). The two simultaneous pulses are equivalent to an amplitude-modulated pulse applied on-resonance to the middle and in the form of

$$\mathcal{H}(t) = 2f_1 I_x \cos(2\pi\Delta t), \quad 0 \leq t \leq t_w, \quad [29]$$

where $2\pi f_1 t_w = \pi$ is required for an inversion at Δ or $-\Delta$ and the amplitude of the pulse is $2f_1$ because of the interference between the two pulses. To have a zero excitation in the middle, the amplitude-modulated pulse must satisfy the relationship,

$$2\pi\Delta t_w = j\pi, \quad j = 1, 2, \dots, \quad [30]$$

which leads to a zero-order average Hamiltonian,

$$\bar{\mathcal{H}}^{(0)} = \frac{1}{t_w} \int_0^{t_w} 2f_1 I_x \cos(2\pi\Delta t) dt = 0. \quad [31]$$

Since $[\mathcal{H}(t'), \mathcal{H}(t'')] = 0$, all the higher-order average Hamiltonians vanish. As a result, the middle point remains unexcited no matter how strong the pulse is.

For a small offset δ (measured from the middle), the Hamiltonian in Eq. [29] should also include an offset term δI_z , i.e.,

$$\mathcal{H}(t) = 2f_1 I_x \cos(2\pi\Delta t) + \delta I_z. \quad [32]$$

It can be shown that the RF pulse term in Eq. [32] is averaged to

zero over the time of t_w , and the first-order average Hamiltonian,

$$\overline{\mathcal{H}}^{(1)} = \frac{-i}{2t_w} \int_0^{t_w} dt_2 \int_0^{t_2} [\mathcal{H}(t_2), \mathcal{H}(t_1)] dt_1 = 0, \quad [33]$$

for $j = 2$ (Eq. [30]). Consequently, a compensation in the middle with a similar range as in Fig. 6b is formed. The inversion profiles at Δ and $-\Delta$, however, are not compensated at all. The other disadvantage of this scheme lies in that it requires twice the amplitude of the RF pulse.

For $j = 1$, one can show that $\overline{\mathcal{H}}^{(1)}$ is no longer zero and f_1 must be increased two fold to meet the inversion condition ($2\pi f_1 t_w = \pi$). As a result, the compensation in the middle vanishes almost completely.

CONCLUSIONS

The evolution of a spin system by a pulse sequence of PIPs can be calculated in the eigenframe, where the strength of the PIP for the center band is scaled by a factor of $\lambda = \sqrt{2[1 - \cos(\Delta\varphi)]}/|\Delta\varphi|$ and the phase of the PIP is shifted by the UPS = $-\Delta\varphi/2$. The phase differences between different eigenframes can be attributed to the initial phase of the PIPs, making it possible to use the Bloch vector model even in different eigenframes. The effective offsets, however, are different in different eigenframes and the final density operator needs to be transferred back to the rotating frame only at the end of the sequence.

Due to the requirement of the phase inheritance, the order of the PIPs in a pulse sequence is usually fixed even for symmetrical excitation as shown in Fig. 6d.

At very high field, the $^{13}\text{C}_\alpha$ and ^{13}CO chemical shift regions for protein backbones, with a 118-ppm difference between the two centers, can be excited separately and coherently, one with the normal RF pulses in the rotating frame and the other with the PIPs in the eigenframes.

The idea of coherent excitation provides a rigorous solution for pulse sequences with PIPs. It is quite helpful in designing multidimensional NMR sequences at very high field when coherent excitations of multibands are necessary, especially in the ^{13}C channel. Almost all the existing methods (18), developed in the rotating frame, such as coherence and population transfers (19–22), selective excitation (23–28), composite pulses for decoupling (29, 30), and isotropic mixing (31–33), etc., can all be achieved in the eigenframes using the PIPs. In addition, it also introduces a new way to construct composite pulses with not only amplitude and phase modulations but also offset modulation. Moreover, the evolution of the density operator in the eigenframes as described by Eq. [13] can be treated further by using the well-known coherent average theory (34), making the calculation even more convenient for some sequences of multiple PIPs.

ACKNOWLEDGMENTS

This research was supported by NIH (AI27744), NIEHS (ES06676), the Welch Foundation (H-1296), the Lucille P. Markey Foundation, and the Sealy and Smith Foundation. Building funds were provided by NIH (1CO6CA59098).

REFERENCES

1. G. Drobny, A. Pines, S. Sinton, D. Weitekamp, and D. Wemmer, *Faraday Div. Chem. Soc. Symp.* **13**, 49 (1979).
2. A. A. Bothner-By and J. Dadok, *J. Magn. Reson.* **72**, 540 (1987).
3. H. Geen, X. Wu, P. Xu, J. Friedrich, and R. Freeman, *J. Magn. Reson.* **81**, 646 (1989).
4. L. E. Kay, D. Marion, and A. Bax, *J. Magn. Reson.* **84**, 72 (1989).
5. S. L. Patt, *J. Magn. Reson.* **96**, 94 (1992).
6. S. Zhang and D. G. Gorenstein, *J. Chem. Phys.* **105**, 5659 (1996).
7. L. E. Kay, M. Ikura, and A. Bax, *J. Magn. Reson.* **89**, 496 (1990).
8. A. L. Davis, R. Boelens, and R. Kaptein, *J. Biomol. NMR* **2**, 395 (1992).
9. D. R. Muhandiram and L. E. Kay, *J. Magn. Reson. B* **103**, 203 (1994).
10. T. Szyperski, D. Braun, C. Fernandez, C. Bartels, and K. Wüthrich, *J. Magn. Reson. B* **108**, 197 (1995).
11. A. Abragam, "Principle of Nuclear Magnetism," Oxford Univ. Press, Oxford (1961).
12. M. Mehring, "High Resolution NMR Spectroscopy in Solids," Springer-Verlag, Berlin (1976).
13. U. Haebleren, "High Resolution NMR in Solids: Selective Averaging," *Advances in Magnetic Resonance*, Suppl. 1. Academic Press, New York (1976).
14. M. H. Levitt and R. Freeman, *J. Magn. Reson.* **33**, 473 (1979).
15. E. L. Hahn, *Phys. Rev.* **80**, 580 (1950).
16. M. A. McCoy and L. Mueller, *J. Magn. Reson.* **98**, 674 (1992).
17. S. Zhang and D. G. Gorenstein, *J. Magn. Reson.* **132**, 81 (1998).
18. R. R. Ernst, G. Bodenhausen, and A. Wokaun, "Principles of Nuclear Magnetic Resonance in One and Two Dimensions," Clarendon, Oxford (1987).
19. G. A. Morris and R. Freeman, *J. Am. Chem. Soc.* **101**, 760 (1979).
20. S. R. Hartmann and E. L. Hahn, *Phys. Rev.* **128**, 2042 (1962).
21. O. W. Sørensen, *Prog. NMR Spectrosc.* **21**, 503 (1989).
22. S. Zhang, P. Xu, O. W. Sørensen, and R. R. Ernst, *Concepts Magn. Reson.* **6**, 275 (1994).
23. W. S. Warren, *J. Chem. Phys.* **81**, 5437 (1984).
24. R. Freeman, *Chem. Rev.* **91**, 1397 (1991).
25. J. Baum, R. Tyko, and A. Pines, *J. Chem. Phys.* **79**, 4643 (1983).
26. W. S. Warren and M. S. Silver, in "Advances in Magnetic Resonance," Vol. 12, p. 248, Academic Press, San Diego (1988).
27. G. Bodenhausen, R. Freeman, and G. A. Morris, *J. Magn. Reson.* **23**, 171 (1976).
28. S. Zhang and D. G. Gorenstein, *Chem. Phys. Lett.* **303**, 587 (1999).
29. M. H. Levitt, R. Freeman, and T. Frenkiel, *J. Magn. Reson.* **47**, 328 (1982).
30. A. J. Shaka and J. Keeler, *Prog. NMR Spectrosc.* **19**, 47 (1987).
31. L. Braunschweiler and R. R. Ernst, *J. Magn. Reson.* **53**, 521 (1983).
32. A. Bax, D. G. Davies, and S. K. Sarkar, *J. Magn. Reson.* **63**, 230 (1985).
33. A. J. Shaka, C. L. Lee, and A. Pines, *J. Magn. Reson.* **77**, 274 (1988).
34. U. Haebleren and J. S. Waugh, *Phys. Rev.* **175**, 453 (1968).